IN SITU SPECTROELECTROCHEMICAL TECHNIQUES IN ELECTROCHEMISTRY

A. Hamnett, P.A. Christensen and S.J. Higgins

Inorganic Chemistry Laboratory
South Parks Road
OXFORD OX1 3QR

Abstract

Electrochemistry is on the threshold of a new era of expansion as information from novel spectroelectrochemical techniques is brought to bear on the faradaic processes taking place at electrodes.

In this paper, the bases of two important techniques, ellipsometry and *in situ* FTIR reflectance spectroscopy, are described, and their application to a number of problems is reviewed.

The first problem investigated is the adsorption and orientation of molecules on surfaces. Applications of the two techniques to problems of electrochemical promotion and polymer precursors are described.

The second problem covered is the mechanism of oxidation of methanol on dispersed platinum catalysts. The evidence will be reviewed for the importance of oxide poisoning in practical systems. Data from FTIR, X-Ray Photoelectron spectroscopy and Moessbauer spectroscopy will then be summarised and the possible mechanisms for ruthenium promotion of platinum discussed in the light of the evidence.

Finally, the problem of the growth of electroactive polymers on surfaces, is addressed, taking as example the growth and potential cycling of Prussian Blue films on platinum.

Pleanary lecture delivered at the 4th Meeting of the Portuguese Electrochemical Society, Estoril, March 1989

Portugaliæ Electrochimica Acta, 7 (1989) 591-618

Introduction

The weapons in the hands of the professional electrochemist are increasing in number and sophistication at an extraordinary rate. The forties and fifties of this century saw the establishment of methods for the control of the transport of solution species from the bulk solution to the electrode, and the development of true hydrodynamic techniques in the sixties allowed us to detect unstable solution intermediates at auxiliary electrodes. Although this permitted the study of complex EC and ECE reactions, surface-trapped intermediates remained inaccessible by direct observation, and inferences from increasingly complex potential pulse, cycling and a.c. experiments were employed to understand such problems as electrocrystallisation, anodic oxidation of organic molecules and polymer growth. It has, however, long been recognised that such data is inferential: it is possible to *eliminate* kinetic schemes by comparison of the predicted and observed iV/t behaviour, but it is never possible unambiguously to *prove* that a complex mechanism derived from purely kinetic data is the only one consistent with experiment.

These difficulties have been recognised for a long time, but the liquid/solid interface has not proved amenable to study by molecular spectroscopic techniques, at least *in situ*. The immense revolution in the study of the gas/solid interface that followed on the development of electron spectroscopy and microscopy has only been applicable to electrodes after emersion and evacuation, a fact that has severely limited the usefulness of this type of technique. It is not possible to apply electron spectroscopic methods *in situ* to the liquid/solid interface as the mean free path of electrons in a condensed phase is extremely low. Furthermore, the application of *in situ* IR appeared doomed by the very high cross-section for absorption of IR by water and other common protic solvents. The cross-section for Raman was thought to be too low for any practicable purposes and electroreflectance techiques were bedevilled by instrumental and interpretative problems, as was ellipsometry.

The last fifteen years have seen major changes in this prognosis. The arrival of automatic ellipsometers has enormously facilitated measurements by this technique[1] and the development of powerful microcomputers has allowed us to process the data far more rapidly and conveniently. In-situ IR has been shown to be both feasible and to have the sensitivity to detect sub-monolayer amounts of surface-trapped intermediates in favourable cases[2,3]. The theoretical basis of electroreflectance has been substantially extended[4] and, most remarkably, Raman spectra from specially roughened surfaces have been measured and interpreted to yield information on adsorbed molecular orientation[5]. Even direct structural tools have begun to be exploited: low-angle X-ray and neutron scattering have been used to study long-range order on surfaces[6] and, perhaps most excitingly, Scanning Tunnelling Microscopy has begun to be applied to the liquid/solid interface to give direct real-space images *in situ*[7].

It is becoming apparent as a result of the development of these techniques that many surfaces have a rich chemistry that is all but inaccessible by iV/t measurements. The direct identification of adsorbed species by their IR or Raman spectra, the direct measurement of kinks and critical clusters in electrocrystallisation and the direct observation of pits in corroding iron are all now feasible. This paper addresses itself to the study of well-defined films on surfaces, and it is reasonable to ask what information is desirable in the study of such films. A preliminary list might be:

1. The conditions of formation
2. The film composition (*eg* presence of solvent, counterions *etc*)
3. The film thickness and its porosity or microstructure
4. The mechanism of film formation and growth
5. Any kinetic limitations on growth
6. The physical properties of such films (optical, electronic *etc*)
7. The electrochemical cycling properties
8. Any changes in composition and thickness on potential cycling
9. Any changes in physical properties on potential cycling
10. The stability to cycling and the modes of film decay

There are few if any systems for which information in all of the above categories is available, and it is clear that much of this information can only be provided by techniques that transcend the purely electrochemical. In order to illustrate the use of some of the new spectroelectrochemical methods, three examples have been chosen from our recent measurements and these are described in the paper. Initially, some background information on ellipsometry is provided, followed by a discussion of its applications to the adsorption of monolayers, then *in situ* FTIR is reviewed with applications to methanol oxidation and finally both techniques are applied to Prussian Blue.

Ellipsometry

Several techniques have been applied to the problem of film *thickness*, referred to by Greef as the "missing dimension" of electrochemists[8]. These include:

1. Optical absorbance measurements

In order to relate these to film thickness, the value of the absorption coefficient must be known, and there must be no unknown contribution from the solution layer sampled by the beam. In general these conditions are difficult to fulfil.

2. Interferometry

The film thickness must, under normal circumstances, be comparable to the wavelength of the incident beam for this technique to give accurate results. It becomes substantially less accurate for film thicknesses below *ca.* 1000 Å

3. Ellipsometry

This is extremely sensitive and can yield film thickness and optical properties simultaneously. There are, however, problems with interpretation, including assumptions about roughness and uniformity of films that sometines make the conclusions controversial.

The basis of ellipsometry has been discussed by Greef[8], who defined ellipsometry as: "the analysis of the change in polarisation state of a light beam when it is reflected from a surface". When plane polarised light is reflected from a surface, the resultant light beam is, in general, *elliptically* polarised. The angle that this ellipse makes with the *plane of reflection* is termed the azimuthal angle, α, and the the eccentricity, ε, of the ellipse is defined as arctan(b/a), where b and a are the minor and major axes of the ellipse. These angles can be measured with considerable precision. From them, the (complex) reflectivity ratio of the surface can be calculated:

$$\rho = r_{\parallel}/r_{\perp} = \tan(\Psi)\exp(i\Delta)$$

where

$$\tan(\Psi) = \tan(P)/\tan(b) \quad \text{and} \quad \tan(\Delta) = \tan(2\varepsilon)/\sin(2\alpha)$$

and P is the angle made by the direction of polarisation of the light with the plane of reflection, and the angle b is defined by the relations

$$\sin(2b) = \sin(2\varepsilon)/\sin(\Delta)$$
$$\tan(2b) = \tan(2\alpha)/\cos(\Delta)$$

In addition, the *intensity* of the reflected light, $I = I_r/I_o$, can be measured in certain types of automated ellipsometry.

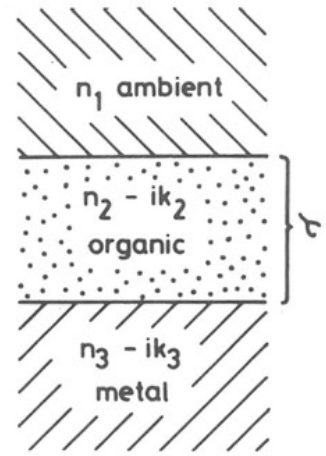

Fig. 1 Three-phase model for intepretation of results

Interpretation of ellipsometric results is commonly based on the three-phase model shown schematically in fig.1. Normally, the refractive index

of the ambient medium, n_1, is assumed known and *real* (that is, the ambient medium is assumed to be non-absorbing). Similarly, the (complex) refractive index of the underlying substrate (usually metallic in an electrochemistry experiment) is assumed known or measurable. This leaves us with the unknown film, and it is evident that *three* parameters are necessary to define the ellipsometric response of a uniform film: these are the *real* part, n, of the refractive index, the *imaginary* part, k (related to the absorption coefficient of the film), and the *thickness*, τ. By measuring three parameters, one can obtain a single unique solution.

In general, the relationship between n, k and τ and the three experimental parameters Ψ, Δ and intensity, I, is very complex, and progress can only be made by direct computation. However, for thin films on metals having n-values typical of many organic films, it is found qualitatively that changes in Δ reflect changes in film *thickness* whereas changes in Ψ are associated with changes in optical absorbance.

The computation of parameters derived from ellipsometric data involves relatively complex algorithms since the ellipsometric equations themselves cannot be directly inverted. In other words, it is possible to calculate Δ and Ψ from n,k and τ but not to calculate n.k and τ directly from Δ, Ψ, and I. The algorithm shown in fig.2 has been used in our work.

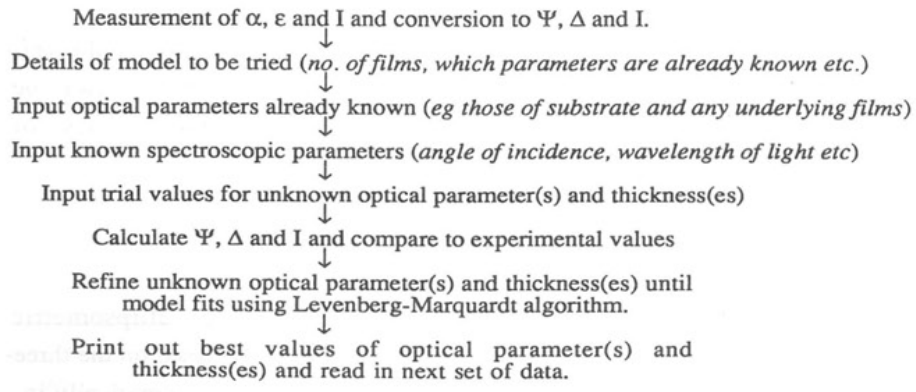

Fig. 2 Algorithm for processing ellipsometric data.

In spite of the fact that light of wavelength *ca.* 5000 Å is used as a probe in ellipsometry, the precision with which the angles Δ and Ψ can be measured makes the technique sensitive to the presence even of monolayers of adsorbate a few ångstroms thick. As an example, we can consider the adsorption of certain classes of molecules discovered by Hill and coworkers[9] to act as promoters for redox protein electrochemistry; these include:

(a) 4,4'-bipyridine and related molecules
(b) PATS-4 and other pyridine thiocarbamates
(c) Thiopyridine and bipyridine-dithiol.

It is thought that these molecules adsorb on the surface of gold or platinum to form monolayers that promote a favourable orientation of the protein with respect to the electrode surface, and it is clear from fig. 3, which shows the change in Δ at different wavelengths following the admission of 1,2-bis(4-pyridyl)ethene that the associated changes in delta greatly exceed the S/N limitations of the instrument. Although less obvious, this is also true of Ψ; a statistical analysis shows that at all three wavelengths, even at 633 nm, the measured changes in Ψ are significant. The measured changes in intensity are, however, too small to be measured by the equipment that we have used, and a unique fit to the experimental data is not possible. In order to make progress[10], values of n_f and k_f were

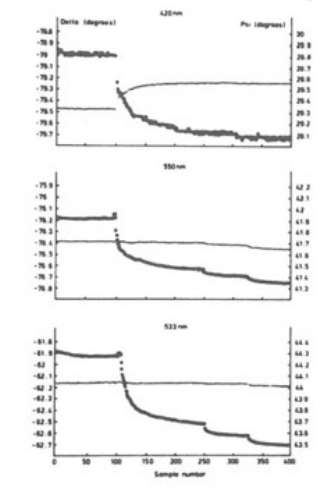

Fig.3 Change in Δ at three wavelengths after addition of BPE

calculated for fixed values of the film thickness τ_f. This thickness was determined for the three molecular orientations shown in fig. 4, and the resultant n_f values were compared to those calculated by using the method of Hubbard *et al.*[11] to estimate the molar coverage, Γ, and employing standard molar refraction theory[12] to estimate n from atomic composition. There is no doubt that the best agreement was obtained for the upright orientation: calculation leads to values of 1.52 (flat or edgewise) and 1.56 (upright), whereas the ellipsometric data leads to values between 2.4 and 3.2 (flat), 1.7 and 1.8 (edgewise) and 1.57 to 1.62 (upright) for n[10].

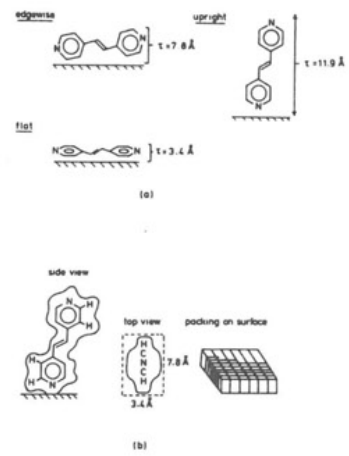

Fig.4 Molecular orientation of BPE derived from ellipsometry.

Several legitimate criticisms of this approach can be made. The most fundamental are:

(a) Is it possible to use essentially macroscopic parameters such as n and k to describe the properties of a monolayer?
(b) The models used imply that the film is strongly anisotropic but the theory pre-supposes an isotropic refractive index.

The first of these is a vexed question and the subject of much debate[13]. It is impossible to give a complete account of the discussion here, but it is known that the pragmatic approach of using the type of calculation outlined above does not appear to lead to inconsistencies. The second problem is more tractable in that theoretical treatments have indicated that a thin axially anisotropic *non-absorbing* film with refractive indices $n_{f\parallel}$ and $n_{f\perp}$ will, if treated as an isotropic film for the purpose

of calculating its optical properties, give a mean pseudo-isotropic refractive index n_f equal to the weighted mean of the anisotropic indices and an absorption coefficient k proportional to the *difference* of the indices[14]. It is, of course, the *mean* refractive index that is calculated from the molar refractivity, and this has, therefore, been adopted as the main method of interpretation.

It is of interest to contrast the behaviour of 1,2-bis(4-pyridyl)ethene with that of 4,4'-dithiodipyridine; in this case, the ellipsometric parameters show changes that initially mimic those of the ethene derivative but then reverse direction. Interpretation of the early part of the adsorption process reveals that adsorption initially takes place with the two S-atoms chemisorbed onto the gold surface; at later times, however, the S–S bond is cleaved and strong chemical interaction between the S atoms and the gold surface takes place.

Redox proteins and especially enzymes are known to adsorb on gold and other metals directly[15], and two examples are shown in figs. 5 & 6. It is clear that adsorption is much slower in these systems both because the concentration of enzyme is much lower than that of promoter (1 μM *vs.* 1 mM) and the diffusion coefficient of proteins is significantly lower. Nevertheless, it is clear that at sufficiently long times, a steady state coverage is reached. The adsorption of cytochrome c peroxidase on graphite is accompanied, at low temperature, by the appearance of electroactivity towards H_2O_2 reduction. It is interesting that this

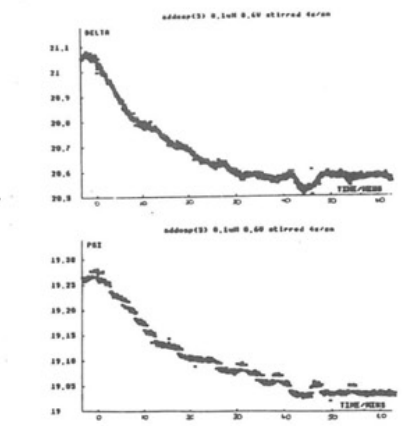

Fig. 5 Changes in Δ and Ψ following admission of 1μM Cytochrome c peroxidase. Electrode is graphite.

electroactivity reaches a limiting value before complete monolayer coverage is attained, a result that can be understood in terms of a model in which each enzyme molecule acts as a miniature microelectrode[16]. The adsorption of bovine serum albumin (fig. 6) shows a curious rise in Δ immediately after addition of the protein; the reasons for this are not yet clear, and further work is planned for this system.

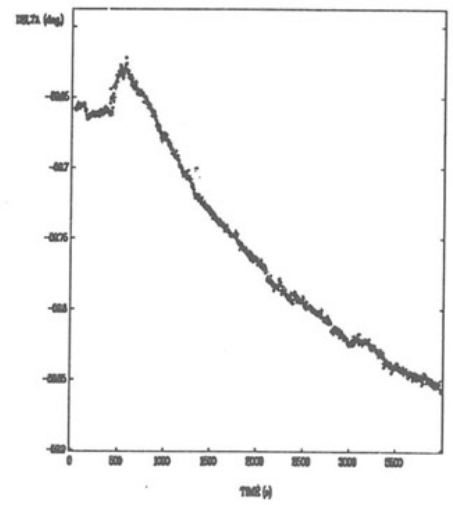

Fig. 6 Change in Δ after admission of bovine serum albumin. Silver electrode.

***In situ* external reflectance FTIR**

As indicated above, until recently *in situ* external reflectance IR was thought to be impracticable at an electrode surface. The spur to its development was undoubtedly the realisation that the information that could be provided would be of immense value in terms of the list detailed in the previous section. The basic information that might be obtained from the technique is:

1. The identification of adsorbed and solution intermediates and products.

2. The elucidation of the reaction mechanisms of processes taking place at the electrode

3. The orientation of adsorbing species.

The basic difficulties facing its experimental realisation are:

(a) Strong absorption by water and other protic solvents

(b) Very high sensitivity and stability needed

(c) The existence of a "surface selection rule" that arises from the fact that E_s has a phase change of π on reflection so $\langle E_s^2 \rangle$ is very small at the surface[3]. Thus

> $\partial\mu/\partial Q_i$ must be $\perp$ to surface for significant absorption.

The very strong absorption by water implies the need for a thin-layer cell, in which the thickness of the electrolyte is kept below *ca.* 1 μm. This leads to severe iR problems, and IR laser studies[17] have shown that for an electrode of 1 cm diameter, almost all the electroactivity is confined to a narrow annulus near the edge of the electrode. In addition, the severely impeded flow of reactants into the layer leads to a rapid depletion of material that can be turned over, a fact that can actually be exploited under certain circumstances.

Stability of the spectrometer is another important problem; at the very least, the spectrometer source should be water-cooled to avoid fluctuations in temperature, and the mirror should be air-driven rather than mechanical. To obtain the necessary sensitivity, an MCT detector is used, and this is cooled by liquid nitrogen, again to avoid temperature fluctuations and to decrease noise. A high-thoughput spectrometer must be used: unless sufficient light is incident on the detector at least to turn over the last significant figure on the A/D converter, no amount of accumulation will be adequate to exploit the advantages of modern FT instruments.

The surface selection rule can also be turned to advantage. In a recent paper, the adsorption of thiophene on platinum in acetonitrile was studied with reflectance IR[18], and the resulting spectra, shown in fig. 7, were

consistent only with adsorption of thiophene at stepped surfaces. Ellipsometry had indicated that thiophene does not adsorb readily on optically smooth platinum, and the IR data shows clearly that it will only adsorb on surface defects. This observation is consistent with the fact that polymerisation of thiophene on scratched platinum electrodes is observed initially to follow the scratch lines.

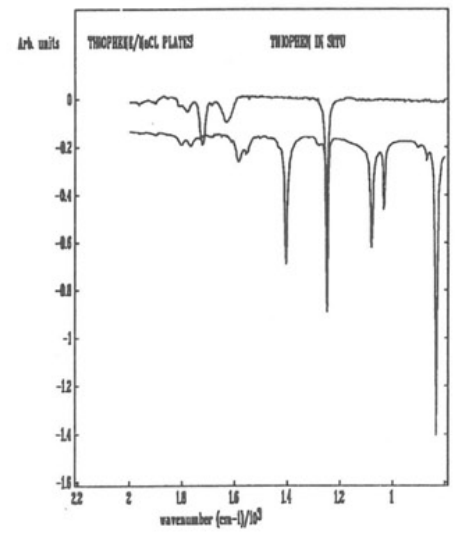

Fig.7 IR spectra of thiophene by transmission (lower) and reflectance (upper).

The fundamental problem in external reflectance IR is to enhance the sensitivity of the technique, especially in aqueous solution, and enhancement bythree methods has been successful[3]:

(a) **EMIRS** - Electrode modulated IR spectroscopy

Apply square-wave modulation and use psd to detect changed response: measure $\Delta\theta/\Delta V$ or $\theta\Delta\nu/\Delta V$.

(b) **SNIFTIRS** - Subtractively normalised FTIR spectroscopy

Advantages:

(1) Multiplex advantage of FT - all radiation from source passes through spectrometer at all times so gain in speed for comparable S/N ratio.

(2) Throughput advantage - no energy dissipating components so higher intensity beam on sample and detector.

(3) Connes advantage: use of internal He/Ne laser as calibrant ensures accurate co-adding and averaging.

(c) **IRRAS** - IR reflection absorption spectroscopy

s-p polarisation modulation to take advantage of surface selection rule.

Of these techniques, EMIRS is extremely sensitive provided that at least one normal mode of an adsorbed molecule has a frequency that is potential-dependent. A well-known example is that of adsorbed CO on platinum, where $\nu(C\equiv O)$ shifts by *ca.* 30 cm^{-1} per volt change in the electrode potential. However, for molecules whose interaction with the surface is weaker, the effect may not be sufficient to obtain a spectrum. The IRRAS technique is, on the face of it, almost ideal: s-polarised light should be blind to surface adsorbed species and substraction of the spectra obtained from p- and s-polarised IR should then yield only the spectra of surface-bound species. Unfortunately, as pointed out by Christensen and Hamnett[3], the reduction in $\langle E_s^2 \rangle$ takes place not only *at* the surface but extends into the electrolyte a distance of the order of the wavelength of the radiation. Thus, in a thin layer cell, subtraction of p- and s-polarised light will lead to a large and uncompensated solution absorbance, which cannot easily be removed.

The most general technique is SNIFTIRS, and we have combined this with a potential step method as follows: in the cyclic voltammogram shown schematically in fig. 8, we can represent by S_n the spectrum collected at potential E_n. The data from a SNIFTIRS run is usually presented as

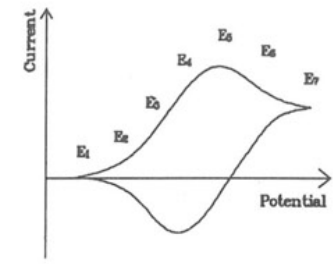

Fig.8 Schematic SNIFTIRS CV

$$\left[\frac{S_n - S_1}{S_n}\right]$$

Thus, features pointing **UP** (to + ΔR/R) correspond to a **LOSS** of absorbing species and features pointing **DOWN** to the **GAIN** of absorbing species as shown schematically for the oxidation of methanol in fig. 9.

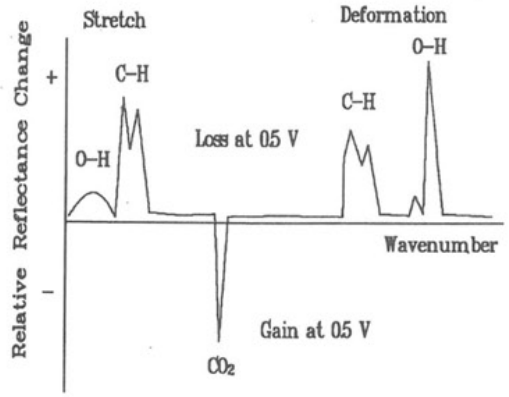

Fig. 9 Schematic SNIFTIRS spectrum for MeOH oxidation

The oxidation of methanol takes place by the reaction:

$$CH_3OH + H_2O \longrightarrow CO_2 + 6H^+ + 6e^-$$

and takes place at potentials greater than 0.4 V *vs* RHE. Thus, in fig. 9, E_b = 0 v and E_w = 0.5 V, where E_b is the base potential and E_w the working potential. The oxidation of methanol has been much studied as a paradigm fuel-cell reaction, and IR results have cast new light on the mechanism of electro-oxidation. The current state of our knowledge of this reaction may be briefly summarised as follows:

(a) At potentials close to 0 V *vs* RHE, adsorption of methanol is very slow and activated[19]. IR data shown in fig. 10 suggest that the main product at this low potential is linearly adsorbed CO.

(b) At higher potentials, some of this adsorbed CO is oxidised to form CO_2; this process commences near 0.4 V *vs*. RHE, as shown in fig. 10.

(c) Above 0.4 V, oxidation of methanol in solution takes two routes depending on the concentration of methanol in the near-electrode region. If this is *high*, then the primary species on the surface is adsorbed CO and this may act both as a poison and an intermediate. If, however, the concentration of methanol is lower, then a three-coordinate intermediate of the form ≡C–OH is formed[20,21], as shown in fig. 11.

(d) If the electrode is held at a potential within the double-layer region and methanol introduced in low concentration, then a totally different surface chemistry is found as shown in fig. 12. Methanol now has to displace adsorbed SO_4^{2-} from the platinum surface and

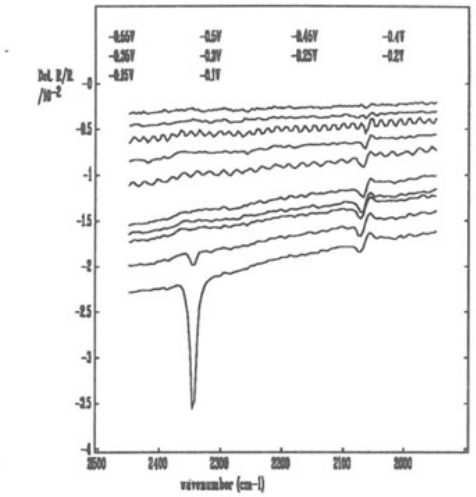

Fig.10 SNIFTIRS spectra of methanol in ν(C≡O) region. Top spectrum: -0.55 V.

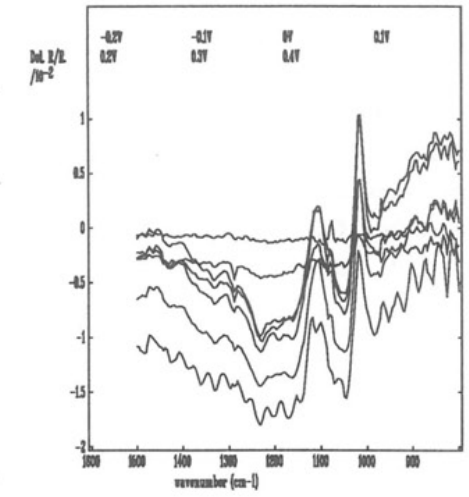

Fig.11 SNIFTIRS spectra of methanol in the ν(C–O) region. Top spectrum: -0.2 V.

apparently adsorbs with the oxygen atoms pointing to the surface to generate a formate-like surface species with peaks at 1400, 2840 and 2955 cm^{-1}. Adsorbed SO_4^{2-} at 1130 cm^{-1} is lost and solution SO_4^{2-} is gained at 1100 cm^{-1}. The difference in behaviour from that found for methanol under normal operating conditions is intriguing; perhaps the presence of adsorbed SO_4^{2-} orients the incoming methanol molecules and nucleophilic substitution then takes place on the surface.

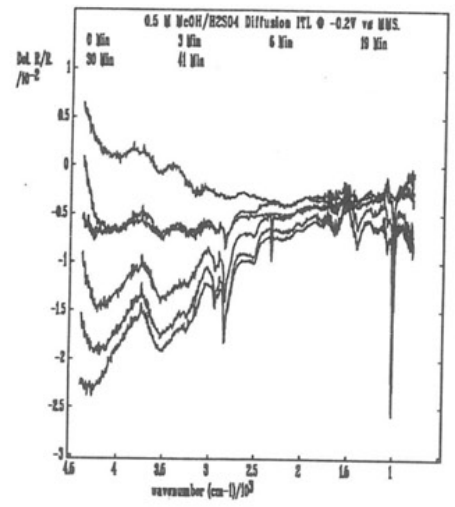

Fig.12 Successive spectra after diffusion of methanol into the thin layer. Top spectrum: 0 min

(e) The behaviour of small platinum particles is apparently rather different from that of planar platinum surfaces. On platinum particles deposited on carbon, no adsorbed CO is seen at all, even though comparable amounts of CO_2 are produced from methanol. There is, however, a peak near 1200 cm^{-1} as shown in figs. 13(a) and 13(b) that behaves as a surface intermediate[20].

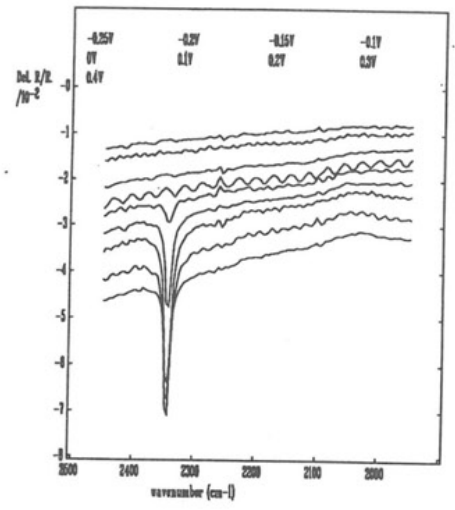

Fig.13(a) SNIFTIRS spectra for methanol oxidation on Pt particles in the ν(C≡O) region. Top spectrum: -0.25 V.

These results have important implications for our understanding of the poisoning of electrodes during methanol oxidation. If planar platinum electrodes are polarised into the double-layer region in the presence of realistic concentrations of methanol in acid, then the current that flows initially rapidly falls to very low levels. This takes place because the platinum surface is rapidly covered with a monolayer of strongly adsorbed intermediate, now believed to be mainly singly or doubly-bonded carbonyl. The coverage of species such as OH_{ads} that can further oxidise these intermediates to CO_2 is very low (i) because the potential is low (ii) the coverage of competing carbonyl species is high.

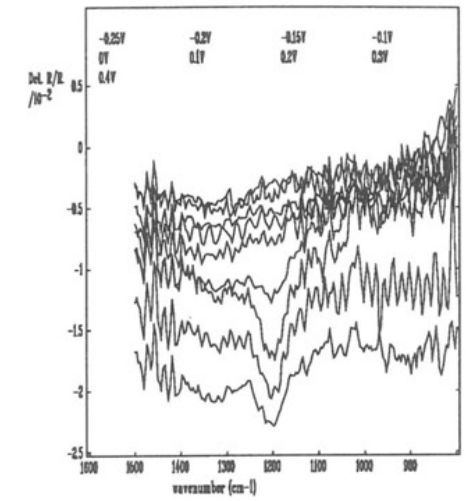

Fig.13(b) SNIFTIRS spectra for methanol oxidation on Pt particles in the ν(C–O) region.

IR results on Pt particles indicate that under conditions of methanol depletion, such as will occur in porous electrodes, these carbonyl species apparently do not form in significant concentrations: a triply bonded *intermediate* is formed that does not cover the whole surface and which can be oxidised by the residual coverage of OH_{ads}.

Although the short-term poisoning of platinum particles is much less serious on porous carbon electrodes, there is a long-term poisoning problem; the following evidence indicates that this *long-term* poisoning arises from the formation of strongly bound oxide groups that are kinetically inert[22]:

(a) No adsorbed CO is found on platinum particles under methanol

depletion conditions in the IR

(b) The XPS of platinised porous-carbon electrodes before and after polarisation indicate increasing amounts of Pt(II) species, as shown in fig. 14.

(c) The lifetime of platinised-carbon electrodes may be significantly enhanced by periodic excursions to open-circuit potential. These excursions may be very short (one minute every two hours), and it is known that such excursions will not reductively eliminate either carbonyl or ≡C–OH intermediates.

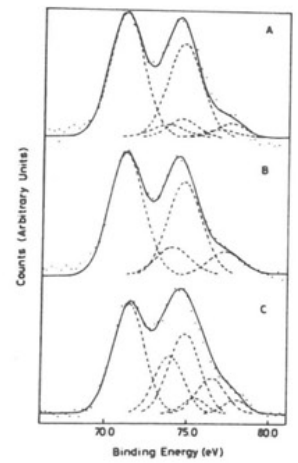

Fig.14 XPS of Pt 4f region for fresh and polarised electrodes showing build-up of apparently *inactive* Pt(II) species.

Platinised carbon, formed into suitably engineered porous electrodes, is highly active for methanol oxidation at potentials above *ca.* 0.5 V *vs.* RHE. Unfortunately, it is not sufficiently active for commercial fuel cell performance and co-promoters have been sought. Most of these promoters operate by one or both of two ways:

(a) They increase the surface coverage of OH_{ads} or other "active" oxide species to enhance the oxidation rate.

(b) They modify the nature of the strongly adsorbed partially oxidised intermediate.

The most effective single promoter is ruthenium, and XPS data indicate that a major effect of ruthenium is to enhance oxide "spillover" onto the platinum and the formation of an apparently *active* form of Pt(II)[23]. Mild promotion is also found for Ir and Os, and XPS data suggest that these are present in part in an oxidised form. By contrast, Pd and Au appear to act as inhibitors, and for both of these, only M(0) is present and no enhancement of Pt(II) is found.

A ^{99}Ru Moessbauer study of Ru/Pt catalysts suggests that most of the Ru in active catalysts is present not as the rutile RuO_2 species but as some form of hydrous oxide that does not show a high quadrupole splitting[24].

A joint FTIR/ellipsometric study on prussian blue

Prussian Blue films can be grown cathodically on a range of electrodes; the main process of growth is though to be:

$$4Fe^{3+} + 3[Fe^{III}(CN)_6]^{3-} + 3e^- = \{Fe_4^{3+}[Fe^{II}(CN)_6]_3\}$$

where the growth solution is 5 mM in $FeCl_3$ and $K_3Fe(CN)_6$ and 1M in KCl. The product is initially the "insoluble" Prussian Blue, but cycling is thought to replace this by the "soluble" form, $KFe^{3+}[Fe^{II}(CN)_6]$.

The following questions can be asked:

(a) Does the film grow homogeneously?
(b) Is there a precursor to the film?
(c) What transformations take place on cycling the film?
(d) Is the film stable to potential cycling?
(e) Is the cycling process kinetically limited in any way?

The following conclusions may be obtained from the ellipsometric data[25]:

(a) Film formation takes place by initial transformation of a precursor

film of Prussian Yellow that has the nominal composition $Fe^{3+}[Fe^{III}(CN)_6]$. The thickness of this film is about 140 Å and this does not change on initial reduction, though there is a pronounced colour change, as shown in the ellipsometric data of fig. 15.

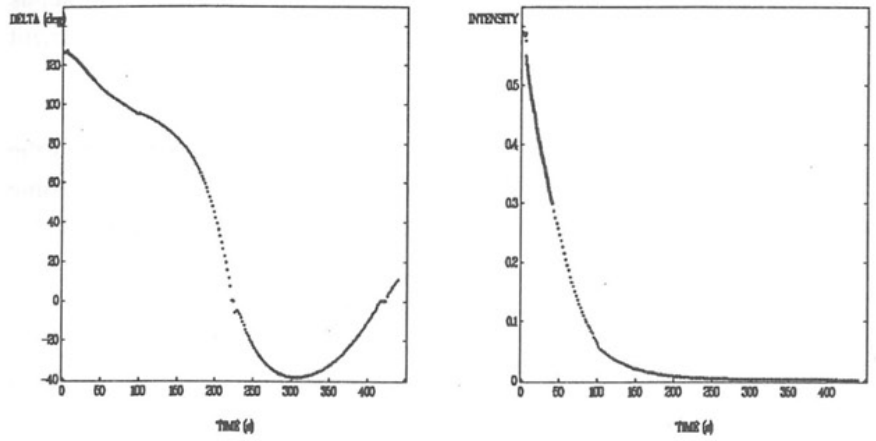

Fig.15(a)&(b) Variation of Δ and I with time during growth of PB film.

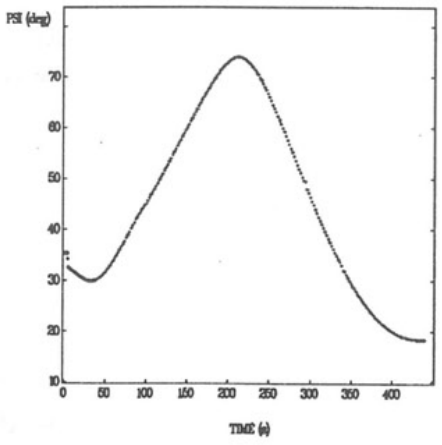

Fig.15(c) Variation of Ψ with time during growth of PB film.

(b) Once steady growth sets in, the intensity falls dramatically. This cannot be understood within the confines of a uniform film model, and the simplest *quantitative* model shows that the film only remains homogeneous up to 1200 Å, with n = 1.424 and k = 0.187. Above this thickness, an outer more porous layer forms with n = 1.345 and k = 0.1 and both films grow steadily. The refractive indices of the outer film suggest extensive hydration.

(c) The final film shown in fig. 15 had an inner layer with n = 1.452, k = 0.253 and thickness 2900 Å and an outer film with the same refractive indices as above and a thickness of 1700 Å. The cyclic voltammogram of this film is shown in fig. 16.

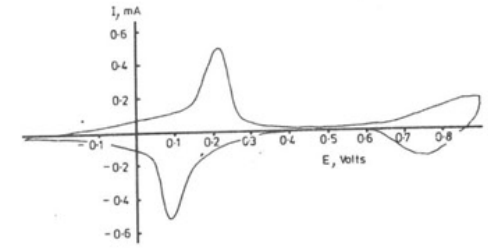

Fig.16 CV of the PB film grown in fig. 15.

(d) On reduction of a well-cycled film, the ellipsometric data of fig. 17 was obtained. This could be interpreted in terms of the inner homogeneous

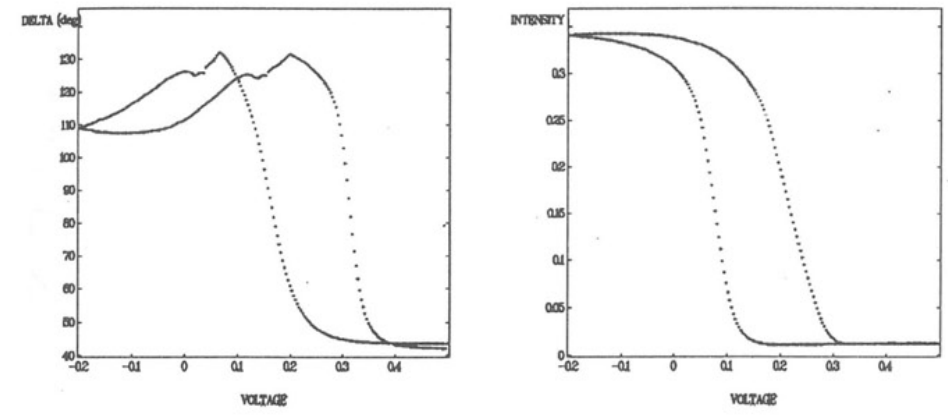

Figs.17(a)&(b) Variation of Δ and Intensity with potential for the transformation PB → PW → PB.

film transforming to a colourless form with n = 1.7 and $k \sim 0$. This transformation is interesting in that it occurred from the electrode *outwards*. The outer film is more difficult to reduce, and is only reduced on the cyclic voltammogram to k = 0.09.

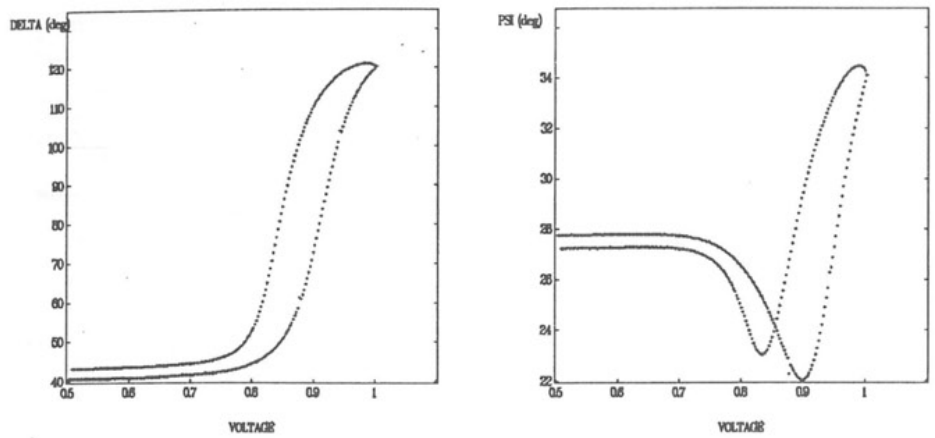

Fig.18(a)&(b) Variation of Δ and Ψ with potential for the transformation PB → PY → PB

(e) On oxidation, a kinetically very sluggish process was observed whose ellipsometric parameters were not entirely reversible as shown in fig. 18. Conversion of the inner film could be modelled assuming that the change was gradual over the entire film, but the outer film was much more difficult to oxidise.

The results of a parallel IR study in which all conclusions are based on the behaviour of the ν(C≡N) stretching modes near 2100 cm^{-1} can be summarised as:

(a) Oxidation of a well-cycled film from PW to PB leads to the gain of a broad peak at 2106 cm^{-1} and a loss peak at 2085 cm^{-1} together with the transient gain near 0.1 V of a peak at 2050 cm^{-1}. This latter appears at -0.2 V, grows to a

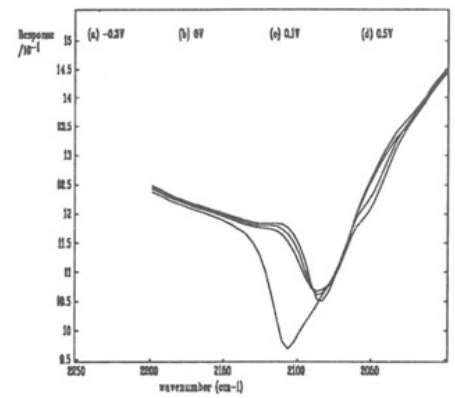

Fig.19 Single-beam spectra in the ν(C≡N) region of PW → PB change.

maximum at +0.15 V and collapses at higher potentials, as can be seen in fig. 19.

(b) Reduction of a well-cycled film of PB to PW follows essentially the reverse of this process, with the 2050 cm^{-1} transient peak again being seen.

(c) If a freshly grown film of PB is reduced, an initially broad band at 2075 cm^{-1} sharpens to a band centred near 2080 cm^{-1}, and a transitory peak is seen at 2106 cm^{-1}, see fig. 20. On re-oxidation a much stronger feature at 2106 cm^{-1} is seen, and the broad peak at 2075 cm^{-1} reappears, together with a transient peak at 2050 cm^{-1}. On further potential cycling, the spectrum of the PB form shows continual growth of the 2106 cm^{-1} band whereas the 2075 cm^{-1} band declines to an ill-resolved shoulder.

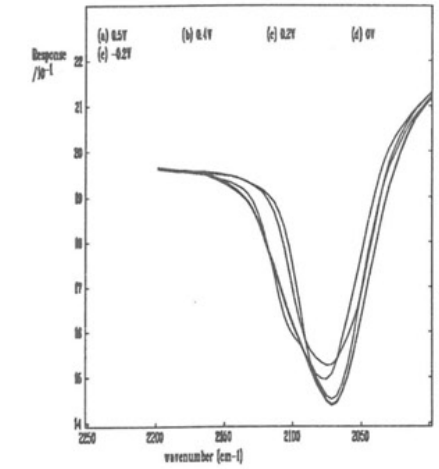

Fig.20. Single-beam spectra in the ν(C≡N) region of PB → PW change for a fresh film.

Taking the ellipsometric and IR data together, the following interpretation of the IR data has been given:

(a) The structure of "insoluble" PB has 1/4 vacancies on the $[Fe^{II}(CN)_6]$ sites. The cyanide bridges associated with these sites are replaced by water molecules, and the resultant structure, shown in fig. 21, is significantly different from the ideal Keggin structure.

(b) Assuming that the final PB spectra are dominated by the "soluble" form, the band at 2106 cm^{-1} must be assigned to the Fe^{II}–C≡N···Fe^{3+} bridge. It is well known that [CN^-] coordinated by N to a cation is blue

shifted, and the 2106 cm^{-1} peak is consistent with a shift of +20 cm^{-1} per unit cation charge as is the assignment of the 2080 cm^{-1} peak to the Fe^{II}–C≡N···Fe^{2+} bridge of PW.

(c) The peak at 2075 cm^{-1} in the initial form of "insoluble" PB can be associated with a Fe^{II}–C≡N··· $[FeOH]^{2+}$ unit, derived from a hydrolysed Fe^{3+} ion.

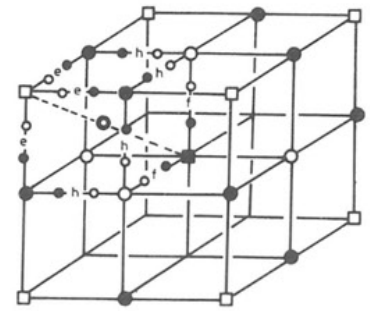

Fig.21 Unit cell of "insoluble" PB

(d) The transformation of "insoluble" to "soluble" forms is apparently driven by the instability of $[Fe^{II}(CN)_6]$ vacancies in the PW form.

(e) The appearance of a transitory peak near 2106 cm^{-1} on reduction of "insoluble" PB can be interpreted as the creation of true Fe^{II}–C≡N···Fe^{3+} bridges. These are formed as a result of the drop in pH associated with an initial influx of protons to effect charge balance (since these are more mobile than K^+).

(f) A transitory peak peak at 2050 cm^{-1} that appears during oxidation can similarly be assigned to the Fe^{II}–C≡N···$[FeOH]^+$ arising from hydrolysis of residual "insoluble" form on re-oxidation. In this case, H^+ ions are expelled preferentially from the film initially.

The following joint conclusions can be stated about the Prussian blue film:

(a) The PB films consists of two layers, and outer porous layer and an inner more compact layer.

(b) The outer layer is kinetically more difficult to oxidise and to reduce than is the inner film: it is initially in the form of "insoluble" PB and this appears to persist over many cycles.

(c) The inner layer is formed initially also of "insoluble" PB but conversion to the "soluble" form takes place, apparently driven by the instability of vacancies in the reduced PW form.

(d) Potential cycling gives rise to marked pH swings in the film associated with the higher mobility of protons.

General Conclusions

This paper reports the results of three different investigations, in each of which the use of *in situ* spectroelectrochemical techniques has led to new insights into the surface chemistry taking place. There can be little doubt that the future development of these techniques, and the appearance of new ones, such as scanning tunnelling microscopy, will continue to have a major impact on electrochemistry. The subject is on the threshold of the same explosion that took place in gas-phase heterogeneous catalysis two decades ago, and it will be an exciting field in which to work.

Acknowledgements

We would like to acknowledge the help of Simon Weeks and Brendan Kennedy in the methanol oxidation work and Rachel Williams, Olwen Lettington and David Elliott in the monolayer adsorption measurements. We would also like to thank David Rosseinsky and Roger Mortimer for helpful advice in avoiding at least some of the pitfalls inherent in research into Prussian Blue films. S.J.H. and P.A.C. thank the SERC for post-doctoral fellowships and we would also like to thank SERC for the purchase of the ellipsometer and MediSense (U.K.) for help towards the purchase of the FTIR spectrometer.

References

1. P.S. Hauge
   Surf. Sci. **96** (1980) 108
2. S. Pons and A. Bewick, *in* Adv. Infra-Red and Raman Spectrosc. **12** (1985) 1; eds. R.J.H. Clark and R.E. Hester, Wiley, London.
3. P.A. Christensen and A. Hamnett, *in* Comprehensive Chemical Kinetics **29** (1989) 1; eds. R.G. Compton and A. Hamnett
4. A. Hamnett, R.L. Lane, S. Dennison and P.R. Trevellick, *in* Comprehensive Chemical Kinetics **29** (1989); eds. R.G. Compton and A. Hamnett
5. M. Fleischmann, P.J. Hendra and J.A. McQuillan
   Chem. Phys. Lett. **26** (1974) 163
6. M. Fleischmann and B.W. Mao
   J. Electroanal. Chem. **247** (1988) 297
7. D.J. Trevor, C.E.D. Chidsey and D.N. Loiacono
   Phys. Rev. Lett. **62** (1989) 929
8. R. Greef in *Comprehensive Treatise of Electrochemistry 8: Experimental Methods in Electrochemistry;* eds. R.E. White, J.O'M. Bockris, B.E. Conway and E. Yeager, Plenum Press, New York, 1984
9. P.M. Allen, H.A.O. Hill and N.J. Walton
   J. Electroanal. Chem. **178** (1984) 69
10. D. Elliott, A. Hamnett, O.C. Lettington, H.A.O. Hill and N.J. Walton
    J. Electroanal. Chem. **202** (1986) 303
11. M.P. Soriaga, P.H. Wilson, A.T. Hubbard and C.S. Benson
    J. Electroanal. Chem. **142** (1982) 317
12. S. Glasstone, *Textbook of Physical Chemistry*, 2nd. Ed., MacMillan and Co. Ltd., London, 1948, p.528
13. See, for example, articles by R.H. Mueller *and* J. Kruger *in* Advances in Electrochemistry and Electrochemical Engineering **9**, eds. P. Delahay and C.W. Tobias, Wiley-Interscience, 1973
14. M.J. Dignam, M. Moskovits and R.W. Stobie
    Trans. Farad. Soc. **67** (1971) 3306
15. B. Ivarsson amd I. Lundström
    CRC Critical Reviews in Biocompatibility **2** (1987) 1

16. F.A. Armstrong, A.M. Bond, A. Hamnett, M. Lannon and O.C. Lettington
    to be published
17. A. Bewick, *private communication*
18. P.A. Christensen, A. Hamnett and A.R. Hillman
    J. Electroanal. Chem. **242** (1988) 47
19. V.E. Kazarinov, G.Ya. Tysyachnaya and V.N. Andreev
    J. Electroanal. Chem. **65** (1975) 391
20. W. Vielstich, P.A. Christensen, S.A. Weeks and A. Hamnett
    J. Electroanal. Chem. Interfac. Electrochem. **242** (1988) 327
21. T. Iwasita and W. Vielstich
    J. Electroanal. Chem. **238** (1987) 383; *ibid* **250** (1988) 451
22. J.B. Goodenough, A. Hamnett, B.J. Kennedy, R. Manoharan and S.A. Weeks
    J. Electroanal. Chem. **240** (1988) 133
23. A. Hamnett and B.J. Kennedy
    Electrochimica Acta **33** (1988) 1613
24. B.J. Kennedy, A. Hamnett and F.E. Wagner
    To be submitted
25. A. Hamnett, S.J. Higgins, R.S. Mortimer and D.R. Rosseinsky
    J. Electroanal. Chem. **255** (1988) 315